Aging of a hard-sphere glass: effect of the microscopic dynamics

2010 J. Phys.: Condens. Matter 22 104121

(http://iopscience.iop.org/0953-8984/22/10/104121)

IOP Publishing Journal of Physics: Condensed Matter

J. Phys.: Condens. Matter **22** (2010) 104121 (6pp) doi:10.1088/0953-8984/22/10/104121

Aging of a hard-sphere glass: effect of the microscopic dynamics

Antonio M Puertas

Group of Complex Fluids Physics, Department of Applied Physics, University of Almeria, 04120 Almeria, Andalucía, Spain

Received 1 October 2009, in final form 1 December 2009
Published 23 February 2010
Online at stacks.iop.org/JPhysCM/22/104121

Abstract

We present simulations of the aging of a quasi-hard-sphere glass, with Newtonian and Brownian microscopic dynamics. The system is equilibrated at the desired density (above the glass transition in hard spheres) with short-range attractions, which are removed at $t = 0$. The structural part of the decay of the density correlation function can be time rescaled to collapse onto a master function independent of the waiting time, t_w, and the timescale follows a power law with t_w, with exponent $z \sim 0.89$; the non-ergodicity parameter is larger than that of the glass transition point (the localization length is smaller) and oscillates in harmony with S_q. The aging with both microscopic dynamics is identical, except for a scale factor from the age in Newtonian to the age in Brownian dynamics. This factor is approximately the same as that which scales the α-decay of the correlation function in fluids close to the glass transition.

(Some figures in this article are in colour only in the electronic version)

1. Introduction

When a fluid is quenched below its glass transition temperature it forms an amorphous solid and exhibits aging, i.e. the dynamics slows down with the time after the quench [1]. This process typically competes with crystallization, which is the equilibrium phase with lowest free energy for simple systems in the region where the glass transition takes place [2]. The slowing down of the dynamics can be noted by the increase of the viscosity or the timescale for structural relaxation, or the decrease of the self-diffusion coefficient. This general scenario is found in both atomic or molecular liquids and colloidal fluids. The latter are particularly interesting since optical techniques can be used to study their dynamics [3]. In addition to the different interactions, the main difference between atomic and colloidal systems relies on the microscopic dynamics, Newtonian in the former, and Brownian in the latter. It was shown by Gleim *et al* [4], however, that the structural relaxation of equilibrium fluids close to the glass transition is identical for both microscopic dynamics. Other structural and dynamical properties are similarly left unchanged by the change of the microscopic dynamics [5, 6].

Using computer simulations, the aging of the mixture of Lennard-Jones (LJ) particles introduced by Kob and coworkers was studied with microscopic Newtonian dynamics [7–9]. This system exhibits a significant slowing down at finite temperature, and the analysis with mode coupling theory (MCT) [11] provided a glass transition at a given temperature T_c [10]. Upon quenching the system below T_c from high temperature the structure evolves very little, whereas the dynamics slows down dramatically. In short, it was found that the density correlation function at different times after the quench, termed 'waiting time', can be collapsed onto a master curve for the structural decay (a stretched exponential), and the timescale for structural relaxation increases with the waiting time following a power law with an exponent slightly smaller than one [7]. Quenches to very low temperatures showed that the relaxation is largely dominated by collective catastrophic events involving a large number of particles [9].

On the other hand, experiments in dense hard colloids have shown a glass transition around a volume fraction $\phi \approx 0.57$ (also obtained via an MCT analysis) [12, 13]. Experimental aging studies in these systems have resulted in moderate agreement with the simulations. Compressed instead of stretched exponential decays were found in the correlation function and the timescale for structural relaxation increased linearly with waiting time [14]. Nevertheless, the glass form factor oscillates in harmony with the structure factor in both experiments and simulations, and is larger than that at the glass point, implying a shorter localization length [15]. Recent results, in contrast, report equilibrated samples of hard colloids above the extrapolated glass transition volume fraction [16], suggesting that the glass transition occurs at a significantly larger density [17].

In this work we study the aging of a quasi-hard-sphere glass by means of simulations, and the effects of using different microscopic dynamics. The system has been studied previously in the fluid regime, and its analysis within MCT yielded a glass transition at a volume fraction $\phi = 0.594$ [5, 18]. Different from the LJ mixture, the only control parameter in this system is the density, reported as a volume fraction, ϕ. Instead of compressing the system instantaneously, our system is prepared at the desired density ($\phi = 0.60$) in the fluid phase, introducing attractions, and at $t = 0$ attractions are removed, following a procedure first used by Foffi *et al* [19]. The results show that the aging in this system is qualitatively similar to that of the LJ mixture, and the different microscopic dynamics introduce only a scaling factor for the waiting time. Interestingly, although the relation between the timescale for structural relaxation and waiting time is not linear, the factor to scale waiting time is similar to that which scales the α-decay of the density correlation function in equilibrium.

2. Simulation details

Computer simulations with microscopic Newtonian and Brownian dynamics (in the canonical ensemble) are run in a polydisperse system of quasi-hard-spheres. The core–core repulsion between particles is designed to be a continuous approximation to the hard-sphere potential:

$$V_c(r) = \epsilon\left(\frac{r}{2a_{12}}\right)^{-36}, \qquad (1)$$

where $2a_{12}$ is the center-to-center distance, $a_{12} = (a_1 + a_2)/2$, with a_1 and a_2 the radii of the particles. To avoid crystallization, the radii of the particles in the simulation are distributed according to a flat distribution centered around $a = 1$ and a half-width of $\delta = 0.1a$. The volume fraction is thus $\phi = (4\pi/3)a^3[1 + \delta^2]\varrho$, with ϱ the number density. In this work, we set $\epsilon = k_BT$, the thermal energy. It has been shown previously that this system behaves effectively as hard spheres (HS), given the high value of the exponent [20].

Both Newtonian and Brownian dynamics simulations were performed to analyze the effect of the microscopic dynamics on the aging of the glass. Newtonian dynamics (ND) was simulated by integrating Newton's equations of motion in the canonical ensemble at constant volume. In Brownian dynamics (BD), or more precisely, strongly damped Newtonian dynamics (dND), each particle experiences a Gaussian distributed white noise force with zero mean, $\vec{\eta}(t)$, and a damping force proportional to the velocity, $\gamma\dot{\vec{r}}$, apart from the deterministic forces from the interactions. Hence the equation of motion for particle j is

$$m\ddot{\vec{r}}_j = \sum_i \vec{F}_{ij} - \gamma\dot{\vec{r}}_j + \vec{\eta}_j(t). \qquad (2)$$

The stochastic and friction forces are linked by the fluctuation-dissipation theorem, $\langle\vec{\eta}_i(t)\vec{\eta}_j(t')\rangle = 6k_BT\gamma\delta(t - t')\delta_{ij}$. The value of γ was set to 50 in units of k_BT, a and m (thermal energy, mean radius and particle mass, respectively). This large value of γ ensures that the particle momentum relaxes in a timescale (m/γ) shorter than the mean collision time (still, a ballistic regime can be identified at very short times). These equations were solved using a Heun algorithm [21]. Both microscopic dynamics (ND and dND) give the same structural relaxation in equilibrium (fluid) states close to the glass transition, as shown previously [4, 5]. In our particular system, a scale factor of 20.5 is needed to collapse the structural decay of the correlation function in dND onto that obtained with ND.

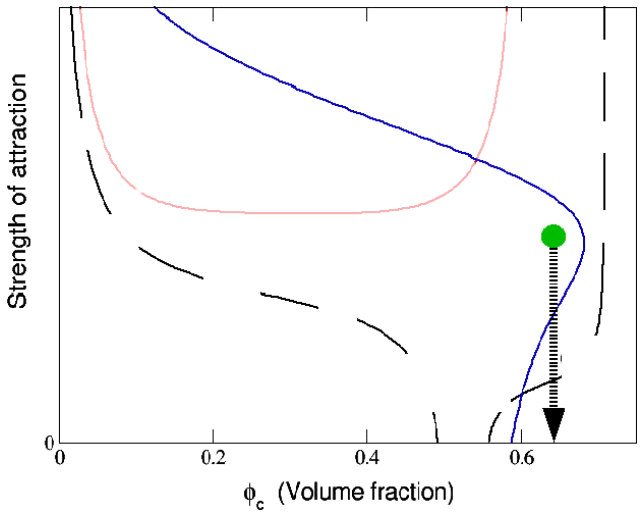

Figure 1. Schematic phase diagram showing the path followed to produce the HS glass. The light red line marks the liquid–gas separation and the broken black line the crystallization boundary—note that crystallization is inhibited in our system. The continuous blue line shows the fluid to glass transition.

In HS there is only one control parameter, namely the number density ϱ, or a coupling between density and temperature in the power potential $\Gamma = \varrho a^3(\epsilon/k_BT)^{1/12}$ [20]; because $\epsilon = k_BT$, the only variations in Γ are due to variations in the density. An HS glass can thus be reached by increasing the density beyond the transition point. However, in order to prepare a glass, a rapid or instantaneous compression from a liquid state creates local stresses and inhomogeneities that can drive the evolution of the system at short times and induce artifacts. We propose here to follow a route making use of short-range attractions. In figure 1 we present the qualitative phase diagram and the liquid–glass transition (continuous dark blue line) in a system with short-range attractions. Note the fluid pocket at high density and moderate attractions between two glasses that can be reached by increasing or decreasing the attraction strength. Foffi *et al* [19] studied the aging of both glasses by an instantaneous quenching or heating. Following a similar argument, we propose here to prepare a high density liquid in this pocket and remove the attractions instantaneously, resulting in the route marked by the thick arrow down to the HS system. If temperature is used as the control parameter, instead of the attraction strength, our route implies raising the temperature to infinity.

In the simulations, the Asakura–Oosawa depletion potential [22] is used with an attraction range $\xi = 0.10a$ and the soft core given above [23]. A system with $N = 1000$

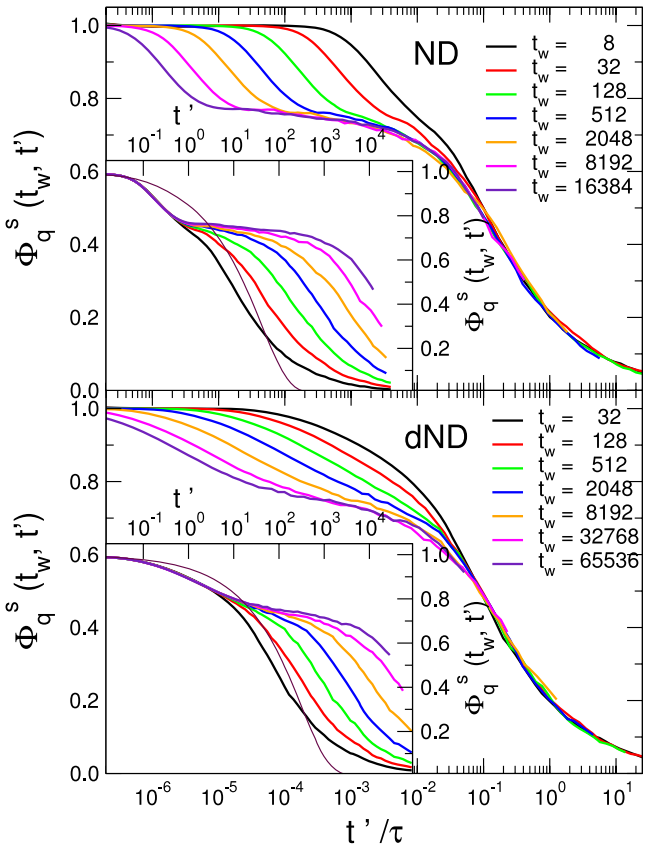

Figure 2. Incoherent density correlation functions (inset) at $qa = 3.8$ (first peak in S_q) and with time rescaled to show the collapse of the α-decay onto a master function (main panels), at different waiting times, as labeled. The thin line in the insets represent the correlation function of the liquid state with attractions. The upper panels correspond to ND, and the lower ones to dND. Note that colors correspond to different waiting times in ND and dND.

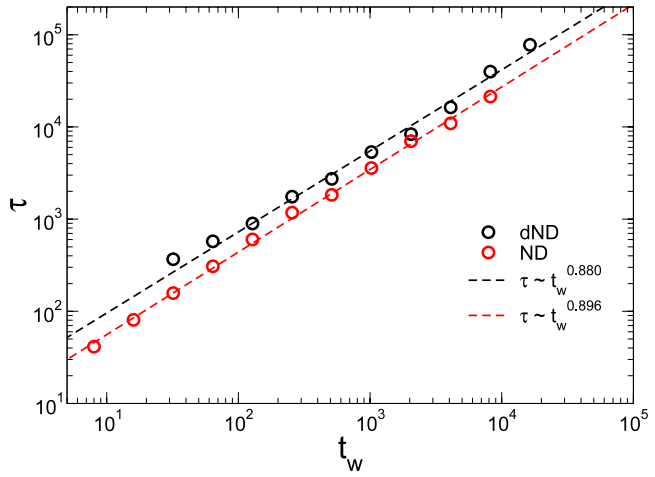

Figure 3. Timescale for the structural decay as a function of the waiting time for both microscopic dynamics (as labeled) used to scale the correlation functions shown in figure 2.

particles is equilibrated at a volume fraction $\phi = 0.60$ and with an attraction strength of $4k_BT$, presented schematically by the green circle in figure 1. At $t = 0$ attractions are instantaneously removed and the system is allowed to evolve with only core–core repulsions at constant volume fraction $\phi = 0.60$. Both microscopic dynamics are used; 100 independent systems are aged with ND and 50 with dND. All dynamical quantities depend on the waiting time, t_w, i.e. the time elapsed after the removal of the attractions, and $t' = t - t_w$; for instance the intermediate scattering function, or density correlation function is $\Phi_q(t_w, t')$ [9].

3. Results

The system at $\phi = 0.60$ with attractions is in the fluid phase because the particles attract each other forming reversible bonds and creating voids that allow the motion of particles and therefore the fluidization of the system. At $t = 0$, the attractions are instantaneously removed and the voids suddenly become crowded. The system starts to age. This aging has only minor effects in the structure of the system, whereas the dynamics is evolving dramatically. The structure factor, S_q, at short waiting time shows the disappearance of the bonds, i.e. the peaks move to smaller wavevectors (larger distances), the neighbor peak grows and the limit $S_{q\to 0}$ decreases (the compressibility decreases). For longer times, no more changes are observed and S_q is constant within the noise level.

The insets to figure 2 show the self-intermediate scattering functions, $\Phi_q^s(t_w, t')$, at different waiting times with both microscopic dynamics. The thin line is the correlation function of the fluid state with attractions, used as the initial state for the preparation of the glasses. Note that the removal of the attractions implies the disappearance of (reversible) bonds, and a concomitant faster relaxation at short times. The aging of the system is then noticed by a slowing down of the structural relaxation, which is observed in both microscopic dynamics. The main panels show that the structural relaxation at different waiting times can be rescaled in time to collapse onto a master decay. This waiting time–time superposition, similar to the time–temperature superposition in equilibrium, has been observed also in other aging systems [7, 24] and indicates that the driving mechanism for structural relaxation does not change, except for the timescale.

The evolution of the timescale for the structural relaxation, τ, defined as $\Phi_q^s(t_w, \tau) = f_q^s/e$, with f_q^s the height of the plateau, is presented in figure 3 as a function of waiting time for both microscopic dynamics. In both cases, τ shows a power law dependence with t_w, and the exponent is the same in ND and dND $z \sim 0.89$. The value of the exponent is, in any case, close to the value found for the LJ mixture [7], $z = 0.88$, also a repulsion driven glass. Because in both microscopic dynamics the same exponent is found, we can conclude that both of them result in the same aging velocity, although microscopic dND causes slower structural relaxation in equilibrium (as mentioned above) and out of equilibrium (see figure 2).

To further explore the similarities in the aging between ND and dND, the structural decays of the correlation functions are directly compared in figure 4. For the same waiting time, an appropriate rescaling of t' leads to a collapse of the plateau region and final decay of the correlation function with ND onto dND. As in equilibrium, this collapse indicates that the

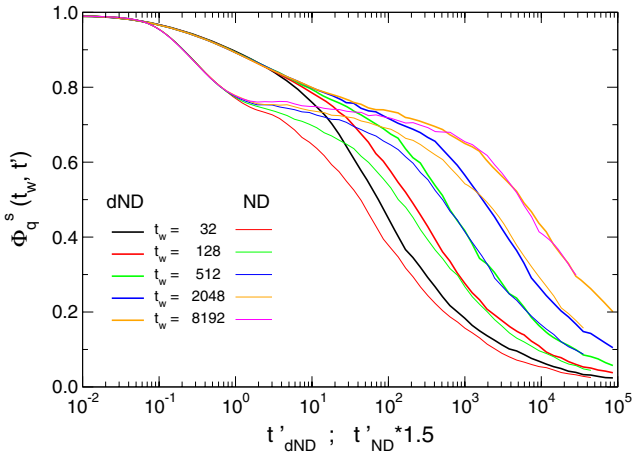

Figure 4. Incoherent density correlation functions for different waiting times with ND and dND microscopic dynamics, as labeled. Time has been scaled to match the α-decay of both dynamics with the same waiting time.

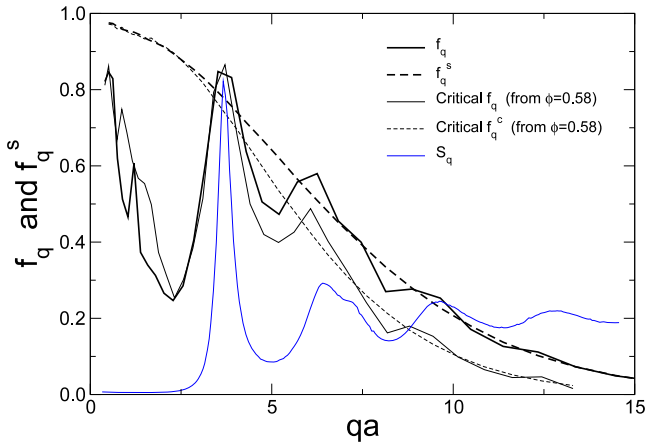

Figure 5. Non-ergodicity parameter (coherent, f_q, and self, f_q^s, parts) and critical parameters obtained from equilibrium simulations at $\phi = 0.58$. The scaled structure factor is also presented showing the oscillations in phase with f_q and f_q^c.

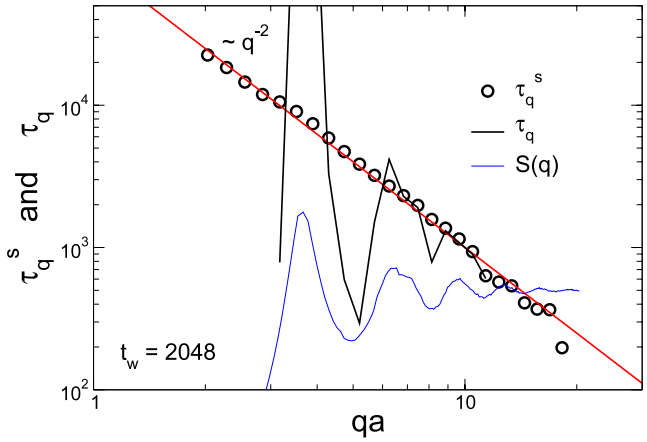

Figure 6. α-timescale for $t_w = 4096$ as a function of the wavevector for the coherent and incoherent correlation functions, black line and circles, respectively. The straight line shows the q^{-2} behavior. The thin line represents the scaled structure factor.

structural relaxation is led by the same mechanisms in both microscopic dynamics. Moreover, the collapse of the structural decay of the correlation function indicates that the master functions in figure 2 are the same.

Since the same structural decays are obtained for different waiting times with both microscopic dynamics, we can write down:

$$\Phi_\alpha^{\mathrm{dND}}(t_{\mathrm{w}}^{\mathrm{dND}}, t'^{\mathrm{dND}}) = \Phi_\alpha^{\mathrm{ND}}(k_1 t_{\mathrm{w}}^{\mathrm{ND}}, k_2 t'^{\mathrm{ND}}) \qquad (3)$$

where the subscript α refers to the structural part of the decay. Making use of the power law relation between τ and t_{w} with exponent $z = 0.89$, the constants k_1 and k_2 must fulfil $k_1^z k_2 = 1.5$, the factor needed to scale functions in figure 4. If we take the value $k_2 = 20.5$ from the equilibrium states close to the glass transition, one obtains $k_1 = 0.053 \approx 1/19$. This implies that $t_{\mathrm{w}}^{\mathrm{dND}} = 0.053 t_{\mathrm{w}}^{\mathrm{ND}}$, i.e. a system of a given age running with dND corresponds to a (19 times) younger system running with ND (judging from their structural relaxations). Interestingly, the intuitive relation $k_1 = k_2^{-1}$, implying that aging and structural relaxation are slowed down in the same way, is obtained approximately although simple aging $z = 1$ is not taking place.

We study now in more detail the properties of the HS glass. The non-ergodicity parameter, f_q, can be obtained from the height of the plateau developed in the intermediate scattering function. As shown in figure 2, f_q is independent of the waiting time, but it is more evident for large t_{w}; we have thus obtained f_q and f_q^s from the largest t_{w}. Both the self- and coherent-non-ergodicity parameters are presented in figure 5 as a function of the wavevector, together with the structure factor S_q and with the critical non-ergodicity parameters obtained from simulations of equilibrium states close to the glass point [5, 18]. Note that f_q in the glass oscillates in phase with S_q and is larger than the critical value, as expected for a system inside the glassy region—except for low wavevectors, where interdiffusion has dramatic effects [18]. Accordingly, the self-non-ergodicity parameter is larger in the glass than the critical value, implying shorter localization length, i.e. there is less space left and the motion of the particles is more hindered. At large wavevectors, the coherent- and self-non-ergodicity parameters coincide.

The wavevector dependence of the correlation functions also provide information about the driving mechanism of the transition by means of the dependence of the timescale. In figure 6 the timescale for the coherent and incoherent correlation functions obtained at $t_{\mathrm{w}} = 4096$ with ND are presented, with the structure factor. For this waiting time the correlation function shows structural slowing down, but decays almost completely in the time window studied here, allowing the measurement of τ_q; qualitatively similar results are obtained, though, for other waiting times. The figure shows that τ_q oscillates in harmony with S_q and the slowest mode is connected with the neighboring peak in S_q. On the other hand, the timescale of the incoherent correlation function follows a power law with the wavevector, with exponent -2, also followed by the coherent timescale at large wavevectors.

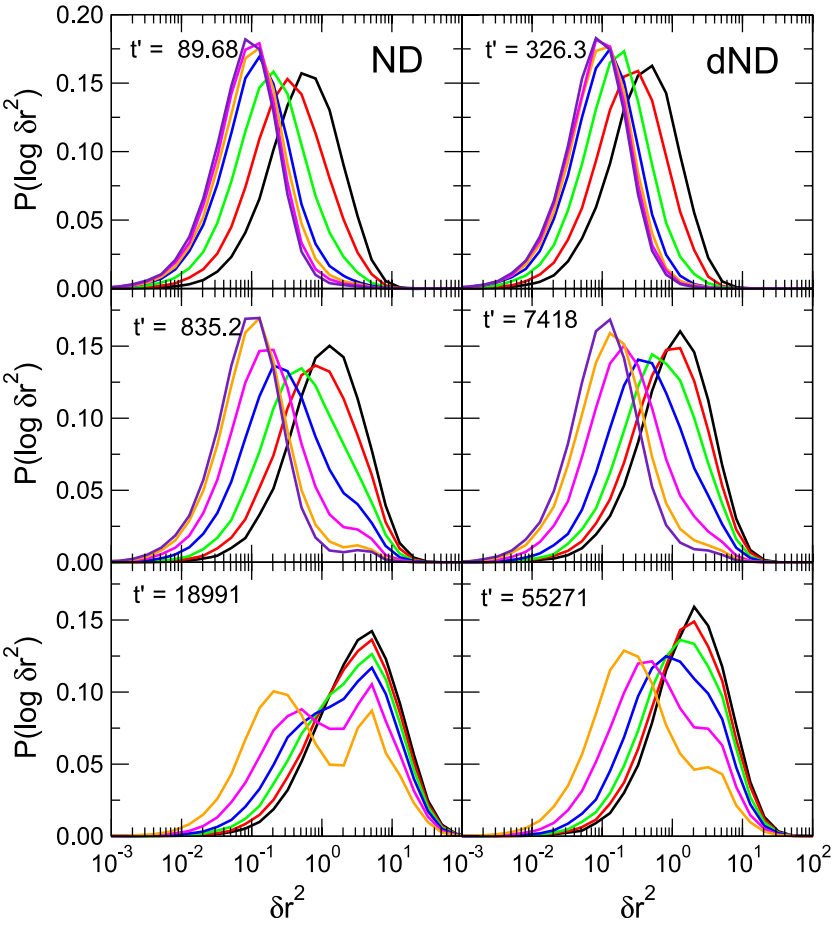

Figure 7. Distributions of squared displacements at different times and microscopic dynamics, as labeled. The different colors indicate different waiting times, with the same code as figure 2. Note that both the time and waiting times are different for ND and dND.

This exponent is also found in the α-timescale of HS fluids close to the glass transition and is connected to the stretching of the correlation function [25].

Finally, we study the distribution of squared displacements in the system, trying to identify dynamical heterogeneities. The distributions shown in every panel of figure 7 are calculated for a constant time after different waiting times, using a logarithmically increasing binning, $P(\log \delta r^2)$—both microscopic dynamics are compared. It is shown there that as the waiting time increases two populations of particles can be identified, according to their mobility. Many particles have moved only a fraction of the diameter, whereas fewer and fewer particles as t_w increases have moved a distance of several diameters. The evolution of the system occurs via a slow displacement of the peak of the slower particles and an increase in the peak of the faster ones. Snapshots of these faster particles show them grouped in elongated clusters that grow with time, resembling the string-like motions observed in dense fluids close to the glass transition. These features can be noticed in both microscopic dynamics—note, however, that the times cannot be compared directly.

Kob and Barrat [9] reported the presence of 'catastrophic events' in the aging of their LJ mixture at low temperatures, in which a substantial portion of the particles (around 10%) move collectively a fraction of the particle diameter. These catastrophic events are not connected with the right peak in the distribution of displacements, which evolves gradually, and have not been noticed in this system. Probably, these can appear at even higher density, where local fluctuations of the stress are more important and release through avalanches.

4. Discussion and conclusions

The temporal evolution of an HS system with a density beyond the MCT-extrapolated glass point has been followed. The findings presented here are similar to the aging of other structural glasses studied by computer simulations; the structural part of the decay of the density correlation function can be time rescaled to collapse onto a master function independent of the waiting time, and the timescale follows a power law with t_w, with exponent $z \sim 0.89$. The non-ergodicity parameter is larger than that of the glass transition point (the localization length is smaller) and oscillates in phase with S_q; also the timescale oscillates in phase with S_q and the slowest mode accessed in the simulations is connected with the neighbor peak. Because the driving mechanism for the transition is the same as in the LJ mixture, similar results are obtained here.

There has been, however, no definitive proof showing that the system at $\phi = 0.60$ is beyond the glass transition and

indeed aging. If the transition point is wrongly estimated by our previous equilibrium analysis [5, 18] as discussed in recent works [16, 17], the system could be 'equilibrating' instead of 'aging'. The simulations presented here, however, do not show any sign of a system reaching equilibrium. On the other hand, the evolution of the non-ergodicity parameter, which is constant in the fluid phase up to the MCT-estimated glass point [5], but increases above it, requires a different theoretical framework from the ideal MCT if the system is to remain in the fluid phase.

Our main result, in any case, concerns the evolution of the system with different microscopic dynamics. It was shown that the structural part of the decay of the density correlation function can be scaled to collapse the dND and ND data onto a single curve. The scaling factor is independent of t_w (and different from 1). Making use of the scaling with the waiting time and the scaling factor between ND and dND in equilibrium, we determine the factor to scale the age in ND with that of dND. Interestingly, this factor is similar to that needed to scale the dynamics in equilibrium. This result could be of interest for future studies of glass aging with simulations, as we have shown and quantified the only effect of using ND or dND.

Acknowledgments

Financial support is acknowledged from the MEC—project MAT2009-14234-CO3-02. I thank Francesco Sciortino and Walter Kob for useful discussions.

References

[1] Angell C A 1995 *Science* **267** 1924
[2] Zaccarelli E, Valeriani C, Sanz E, Poon W C K, Cates M E and Pusey P N 2009 *Phys. Rev. Lett.* **103** 135704
[3] van Megen W and Underwood S M 1993 *Phys. Rev.* E **47** 248
van Megen W and Underwood S M 1994 *Phys. Rev.* **49** 4206
[4] Gleim T, Kob W and Binder K 1998 *Phys. Rev. Lett.* **81** 4404
[5] Voigtmann Th, Puertas A M and Fuchs M 2004 *Phys. Rev.* E **70** 061506
[6] Foffi G, De Michele C, Sciortino F and Tartaglia P 2005 *J. Chem. Phys.* **122** 224903
[7] Kob W and Barrat J-L 1997 *Phys. Rev. Lett.* **78** 4581
[8] Barrat J-L and Kob W 1999 *Europhys. Lett.* **46** 637
[9] Kob W and Barrat J-L 2000 *Eur. Phys. J.* B **13** 319
[10] Kob W and Andersen J C 1995 *Phys. Rev.* E **53** 4134
Kob W and Andersen J C 1995 *Phys. Rev.* E **51** 4626
Kob W and Andersen J C 1994 *Phys. Rev. Lett.* **73** 1376
For a review see Kob W 1999 *J. Phys.: Condens. Matter* **11** R85
[11] Götze W 1999 *J. Phys.: Condens. Matter* **11** A1
[12] Pusey P N and van Megen W 1986 *Nature* **320** 340
Pusey P N and van Megen W 1987 *Phys. Rev. Lett.* **59** 2083
[13] van Megen W, Mortensen T C, Williams S R and Müller J 1998 *Phys. Rev.* E **58** 6073
[14] El Masri D, Pierno M, Berthier L and Cipelletti L 2005 *J. Phys.: Condens. Matter* **17** S3543
[15] Martinez V A, Bryant G and van Megen W 2008 *Phys. Rev. Lett.* **101** 135702
[16] Brambilla G, El Masri D, Pierno M, Berthier L, Cipelletti L, Petekidis G and Schofield A B 2009 *Phys. Rev. Lett.* **102** 085703
[17] Berthier L and Witten T A 2009 *Phys. Rev.* E **80** 021502
[18] Weysser F, Puertas A M, Voigtmann Th and Fuchs M 2010 in preparation
[19] Foffi G, Zaccarelli E, Buldyrev S, Sciortino F and Tartaglia P 2004 *J. Chem. Phys.* **120** 8824
[20] Lange E, Caballero J B, Puertas A M and Fuchs M 2009 *J. Chem. Phys.* **130** 174903
[21] Paul W and Yoon D Y 1995 *Phys. Rev.* E **52** 2076
[22] Likos C N 2001 *Phys. Rep.* **348** 267
[23] Puertas A M, Fuchs M and Cates M E 2002 *Phys. Rev. Lett.* **88** 098301
[24] Puertas A M, Fuchs M and Cates M E 2007 *Phys. Rev.* E **75** 031401
[25] Fuchs M and Mayr M R 1999 *Phys. Rev.* E **60** 5742